ELSEVIER

Journal of Alloys and Compounds 323–324 (2001) 498–503

Journal of ALLOYS AND COMPOUNDS

www.elsevier.com/locate/jallcom

Structural chemistry, magnetic and electrical properties of ternary rare-earth–nickel–phosphides, $R_2Ni_7P_4$ (R=Ce, Pr, Nd)

V. Babizhetskyy, F. Weitzer, K. Hiebl*

Institut für Physikalische Chemie der Universität Wien, Währingerstraße 42, A-1090 Wien, Austria

Abstract

We have investigated the structural chemistry, magnetic and electrical transport properties of ternary compounds $R_2Ni_7P_4$ (R=Ce, Pr, Nd), which crystallize in the orthorhombic $Nd_2Ni_7P_4$ structure-type, space group *Pmn2₁*. The crystal structure for the new compound $Pr_2Ni_7P_4$ has been determined using X-ray powder diffraction data. A least-squares refinement of the atomic positional and thermal parameters by Rietveld method resulted in R_i=0.096 and R_p=0.156, respectively. The Ce and Pr containing samples remain paramagnetic down to 5 K. The cerium atom thereby adopts the ^1S_o configuration due to the tetravalent ground state (Ce^{4+}). $Nd_2Ni_7P_4$ undergoes a ferromagnetic transition at 18 K. The temperature dependence of the resistivities of all three $R_2Ni_7P_4$ compounds resembles the shape of simple metallic conductors. In the paramagnetic region a deflection of the generally linear $\rho(T)$ plot is observed, which could be attributed to the influence of the crystalline field split levels of the degenerate Pr^{3+} and Nd^{3+} ground states. Not knowing the exact 4f level schemes, we use a single spacing (δ) crystal-field model for an order of magnitude estimate.

Keywords: Rare-earth intermetallics; Crystal structure; Electrical transport; Magnetic measurements

1. Introduction

Many ternary compounds of the rare-earth (R=Sc, Y, La–Lu) transition metal (T=3d, 4d and 5d elements) phosphides have been synthesized and structurally identified over the past decades. The magnetic behavior was less intensively studied, the electric transport properties were hardly measured so far [1]. Hence the investigation of the crystal structure and physical properties of the compounds $R_2Ni_7P_4$ [2,3] crystallizing with the $Nd_2Ni_7P_4$ type of structure, became the subject of this research work.

2. Experimental details

Polycrystalline samples of the ternary compounds $R_2Ni_7P_4$ (R=Ce, Pr, Nd) were prepared from pure elements: both red phosphorus and nickel 99.99% supplied by Johnson Matthey (Germany), and rare-earth metal ingots 99.9% by Strem Chemicals. Stoichiometric amounts of powder and filed chips of the constituents were mixed together and pressed into pellets. Prior to the melting in an arc furnace under high purity argon, the pellets were pre-reacted in evacuated silica tubes. The melted buttons were again sealed in evacuated silica tubes, heat treated for 1 month at 1070 K and subsequently quenched by submerging in cold water. Precise lattice parameters and standard deviations were derived by least-squares refinement of room temperature Image Plate Huber G 670 X-ray powder diffractometer data ($8° \leq 2\theta \leq 100°$,stepsize 0.005°) with monochrome Cu $K\alpha_1$. Germanium (99.9999%, a_{Ge}= 0.5657905 nm) served as internal standard.

The magnetic properties were studied by use of a Faraday balance, SUS-10, in the temperature range 80–300 K and in external fields up to 1.3 T and a Lake-Shore AC susceptometer, AC 7000 (f=133.3 Hz, B_{AC}=1 mT) for temperatures 4.2 K<T<100 K.

Measurements of the electrical resistivity were performed applying a common four-probe Lake-Shore AC resistivity option (f=133.3 Hz, i_{AC}=10 mA) in the temperature range 4.2–300 K. The annealed buttons were cut by a diamond saw (Bühler Isomet) into bar-shaped samples with the approximate dimensions of 1×1×5 mm^3. Electrical contacts were made using commercial

*Corresponding author. Tel.: +43-1-4277-52422; fax: +43-1-4277-9524.

E-mail address: kurt.hiebl@univie.ac.at (K. Hiebl).

0925-8388/01/$ – see front matter
PII: S0925-8388(01)01209-9

silver paint (Degussa, Hanau, Germany) and 25-μm gold wire.

3. Results and discussion

3.1. Structural characterization

The X-ray powder patterns of the ternary compounds $R_2Ni_7P_4$ (R = Ce, Pr, Nd) were indexed on the basis of the $Nd_2Ni_7P_4$-structure type [3] orthorhombic unit cell, space group *Pmn2₁*, No. 31. A Rietveld-type profile refinement was performed for the new compound $Pr_2Ni_7P_4$, using the CSD program package [4] to check the crystallographic structure and the atomic positions. Fig. 1 shows the final fit obtained between calculated and observed patterns. Details of the refinement are summarized in Table 1 and final atom parameters are given in Table 2. The projection of the $Pr_2Ni_7P_4$ structure and typical coordination polyhedras (CPs) of corresponding atoms are visualised in Fig. 2. The Pr atoms are surrounded by hexagonal prisms, additional atoms residing off the faces centers (the total coordination number being 20). The nickel atoms are located in the center of orthorhombic prisms with centered square faces, the neighbor atoms of phosphorus form trigonal prisms, respectively. The shortest interatomic distances were observed between Ni and P; d(Ni3–P3) = 2.161(6) Å, d(Ni5–P2) = 2.169(7) Å, d(Ni_7–P1) = 2.161 Å. This finding is typical for the structures of ternary phosphides of rare-earth metals and nickel. The following lattice parameters (Å, $Å^3$) for $Ce_2Ni_7P_4$ (a = 3.7746(7), b = 9.230(1), c = 10.409(1), V = 362.64(1)) and for $Nd_2Ni_7P_4$ (a = 3.7643(3), b = 9.22281(7), c = 10.4096(7), V = 361.39(1)) have been derived. The maximum volume for the praseodymium

Table 1
Rietveld-refinement data of $Pr_2Ni_7P_4$

Formula	$Pr_2Ni_7P_4$
Space group	*Pmn2₁*, No 31
Radiation wavelength Cu Kα_1 (Å)	1.54056
Lattice parameters (Å)	
a	3.77269(4)
b	9.2389(1)
c	10.4335(1)
Unit-cell volume ($Å^3$)	363.67(1)
Calculated density (Mg/m^3)	7.4574(3)
Formula per unit cell	$Z = 2$
Scan range	$8° < 2\theta < 100°$
Step size (2θ)	0.005
Mode of refinement	Full profile
Number of fitted parameters	40
Residual values:	
R_1	0.096
R_p	0.156
R_{wp}	0.105

Table 2
Positional and thermal parameters for $Pr_2Ni_7P_4$

Atom	Position	x/a	y/b	z/c	B_{iso} ($Å^2$)
Pr1	2a	0	0.5641(1)	0.0000	0.80(3)
Pr2	2a	0	0.9384(1)	0.7823(3)	0.95(3)
Ni1	2a	0	0.5846(3)	0.3051(3)	1.05(7)
Ni2	2a	0	0.3256(3)	0.2654(3)	1.57(6)
Ni3	2a	0	0.2541(5)	0.9086(3)	1.06(3)
Ni4	2a	0	0.9008(3)	0.0839(3)	0.95(5)
Ni5	2a	0	0.9363(3)	0.4742(3)	0.96(4)
Ni6	2a	0	0.2802(3)	0.6766(3)	1.21(6)
Ni7	2a	0	0.6946(3)	0.5649(3)	1.05(4)
P1	2a	0	0.5378(5)	0.7186(4)	1.17(11)
P2	2a	0	0.8288(5)	0.2894(6)	1.04(10)
P3	2a	0	0.1586(5)	0.0977(4)	1.11(11)
P4	2a	0	0.1867(5)	0.4645(4)	1.08(12)

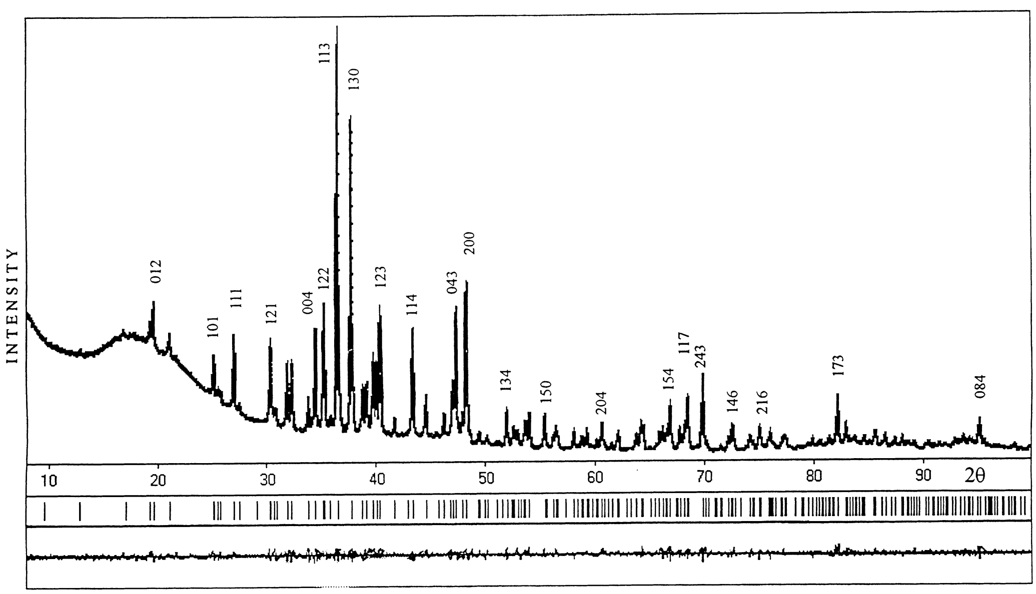

Fig. 1. Observed and calculated profiles of $Pr_2Ni_7P_4$ and their difference plot.

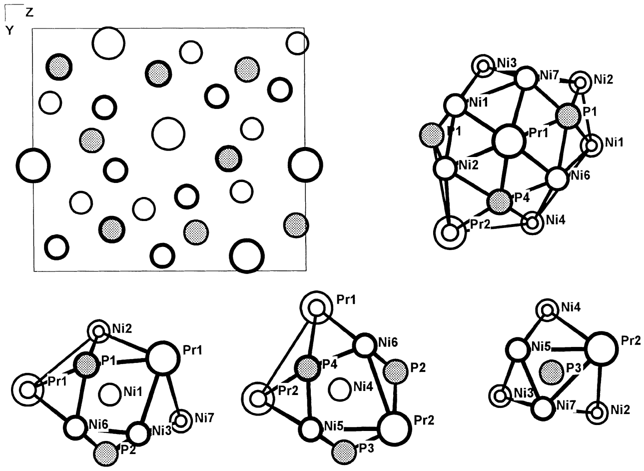

Fig. 2. Projection of the $Pr_2Ni_7P_4$ structure along [001] and typical coordination polyhedra of the atoms.

compound (see Table 1) is a good indication that the cerium ion radius obviously is reduced due to a predominantly tetravalent ground state (see Section 3.2).

3.2. Magnetism

The reciprocal susceptibilities versus temperature for compounds $R_2Ni_7P_4$ are shown in Figs. 3–5. The measured data follow a linear Curie–Weiss law, with the exception for $Ce_2Ni_7P_4$, and the values for the effective moments, μ_{eff}, as well as the paramagnetic Curie temperatures, θ_p, were calculated using the modified formula:

$$\chi = \frac{C}{T - \theta_p} + \chi_o \tag{1}$$

C being the Curie constant and χ_o denotes temperature independent contributions such as core diamagnetism, Landau diamagnetism and Pauli paramagnetism. The derived values in case of the cerium containing compound are: $\mu_{eff} = 0.8\ \mu_B$ $\theta_p = 3$ K and $\chi_o = 1.27 \times 10^{-3}$ cm^3/mol. The reduced moment is an indication that the cerium ion possibly adopts a predominantly tetravalent ground state. It is suggested that the small fraction (<10%) of Ce^{3+} stems rather from secondary impurity phases (note the rise of χ' due to magnetic order below 6 K in inset Fig. 3) than being an intrinsic property. The calculated moments for both compounds $Pr_2Ni_7P_4$ and $Nd_2Ni_7P_4$ (contaminated with small traces of nickel) are in good accord with the theoretical tripositive free ion moments ($\mu_{eff} = 3.5$ and 3.7 μ_B, $\theta_p = -1$ and 2 K). The praseodymium–nickel–phosphide remains paramagnetic in the whole temperature range investigated (see inset Fig. 4). Upon lowering the temperature a maximum in the real part of the dynamic susceptibility curve of $Nd_2Ni_7P_4$ (see inset Fig. 5) is encountered at $T = 18$ K possibly stemming from a ferromagnetic ordering of the Nd^{3+} sublattice.

3.3. Electrical resistivity

The temperature-dependent electrical resistivities of $R_2Ni_7P_4$ are shown in Figs. 6–7 and the $\rho(T)$ curves resemble the typical shape of metal-like intermetallic compounds. Assuming a tetravalent ground state for

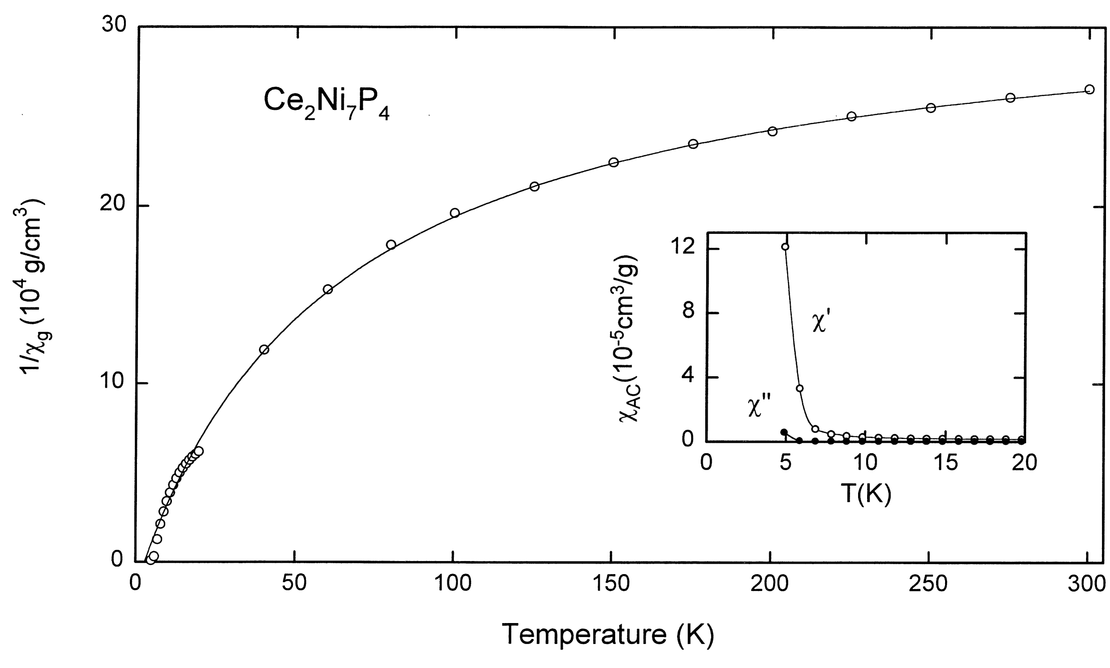

Fig. 3. Reciprocal susceptibility versus temperature for $Ce_2Ni_7P_4$. Solid line calculated according Eq. (1). Inset: dynamic susceptibilities versus temperature.

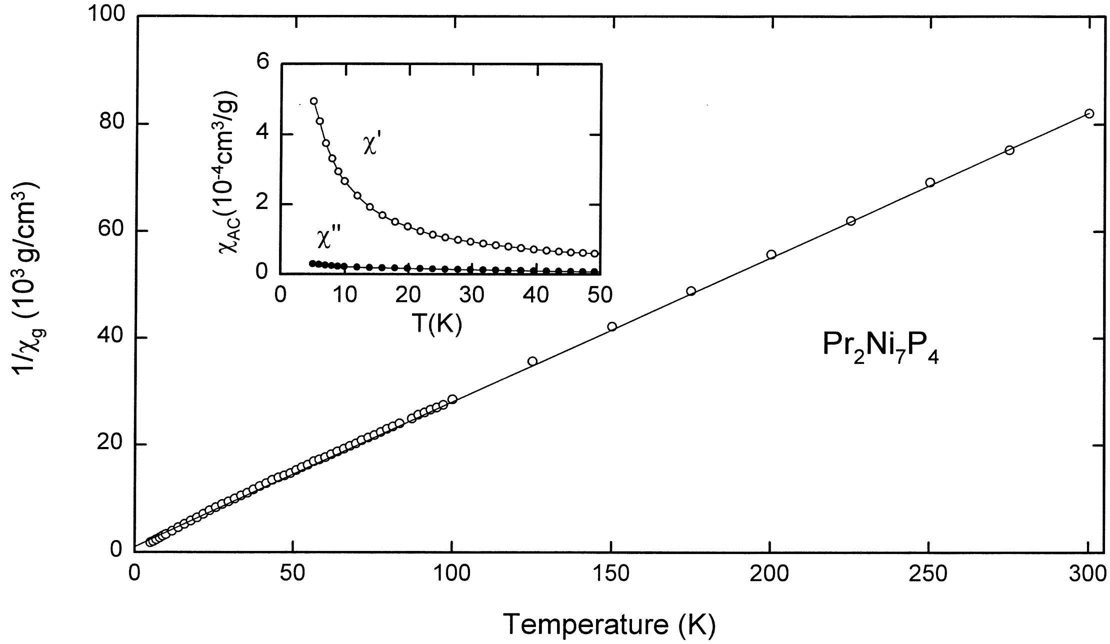

Fig. 4. Reciprocal susceptibility versus temperature for $Pr_2Ni_7P_4$. Solid line calculated according Eq. (1). Inset: dynamic susceptibilities versus temperature.

cerium and the validity of Matthiesen's rule, the resistivity of a non-magnetic compound follows the Bloch–Gruneisen relation [5,6]

$$\rho(T) = \rho_o + 4R\Theta_D\left(\frac{T}{\Theta_D}\right)^5 \int_0^{\Theta_D/T} \frac{x^5\,dx}{(e^x-1)(1-e^{-x})} - KT^3 \tag{2}$$

We have fitted our data according Eq. (2) with the following results: residual resistivity ($\rho_o = 112$ μΩ cm), the second, phonon scattering term, $\rho_{ph}(T)$, ($R = 2.1$ μΩ cm/K, Debye-temperature, $\Theta_D = 99$ K) and the third term, which is due to the scattering of the conduction electrons into a narrow d band near the Fermi level ($K = 9.99 \times 10^{-6}$ μΩ cm/K^3). As can be seen in Fig. 6, the fit is quite excellent. The constant K is rather high, which is an

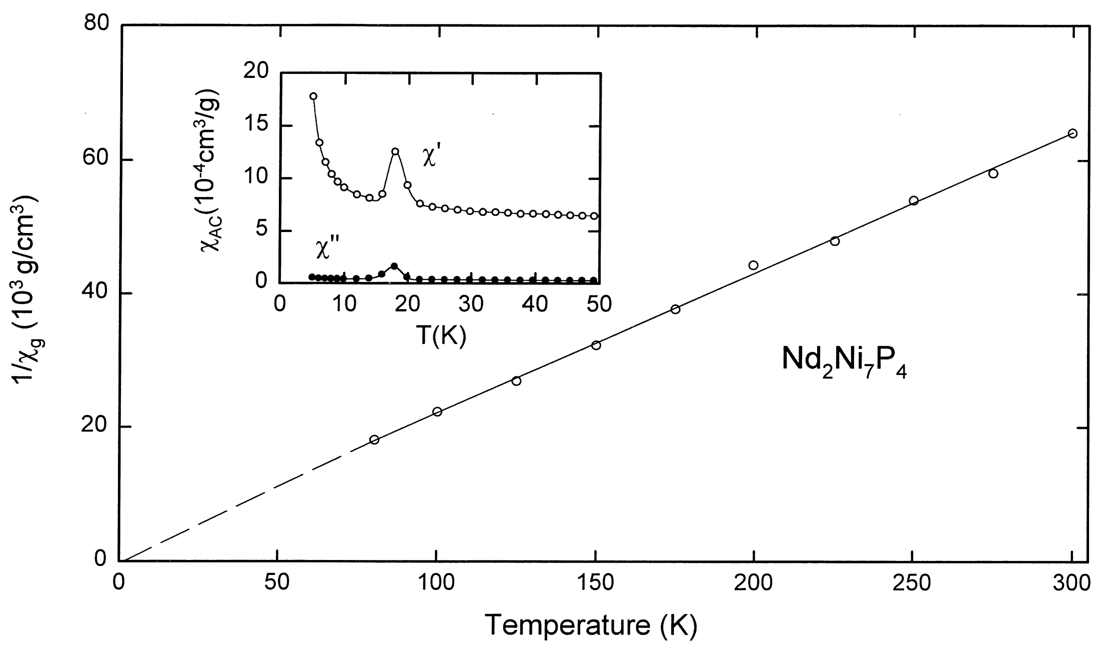

Fig. 5. Reciprocal susceptibility versus temperature for $Nd_2Ni_7P_4$. Solid line calculated according Eq. (1). Inset: dynamic susceptibilities versus temperature.

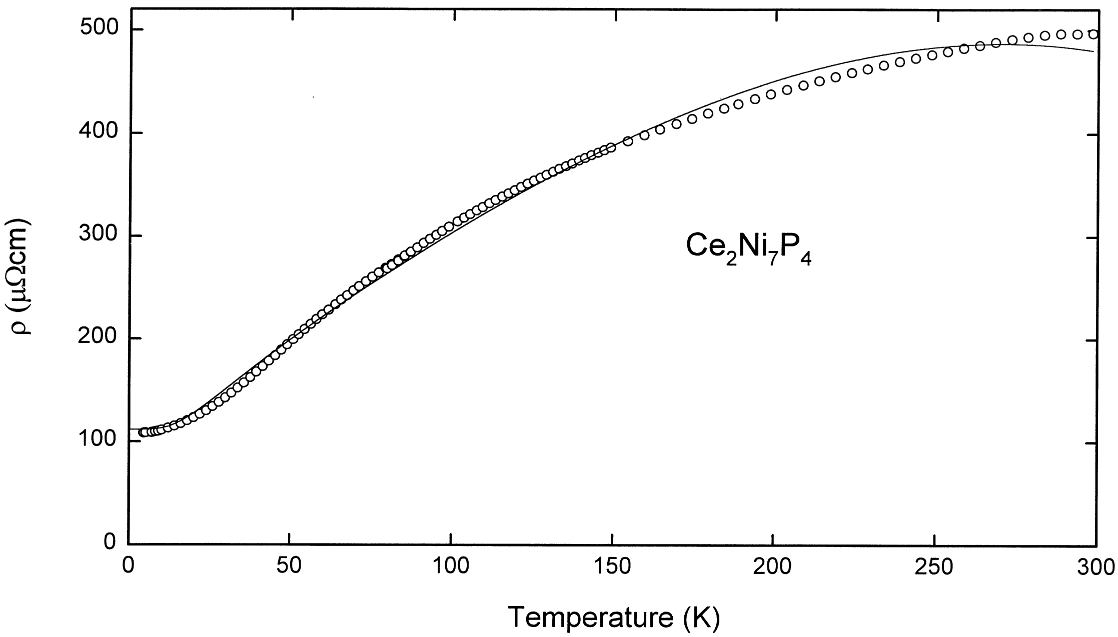

Fig. 6. Electrical resistivity versus temperature for $Ce_2Ni_7P_4$. Solid line calculated according Eq. (2).

indication that the scattering of electrons into such a d band (presumably the Ce 5d) adds an important contribution to the overall resistivity.

The shape of the $\rho(T)$, for $Pr_2Ni_7P_4$ as well as $Nd_2Ni_7P_4$ are very similar. In an enlarged scale the change of slope (see inset Fig. 7) at T_{ord} is visible and a first derivative plot $d\rho/dT$ versus T reveals a shallow maximum at $T_C \cong 18$ K, which is in good accord with magnetic data above. The observed change of slope below 10 K in case of $Pr_2Ni_7P_4$ (see Fig. 7) is possibly owing from an onset of magnetic order, which, however, was not directly detected in $\chi_{AC}(T)$ measurements, but indicated to exist below 5 K, as the χ'' starts to rise in the low temperature regime (see inset Fig. 4). At elevated temperatures ($T > 200$ K) the $\rho(T)$ curves reveal a linear increase owing from a dominant electron phonon scattering process. Upon lowering the temperature $\rho(T)$ decreases more rapidly. In the paramagnetic state it is the influence of the crystal field, which makes the spin disorder resistivity, ρ_{SPD}, temperature dependent. Since a lanthanum containing homologue does not form we tried to

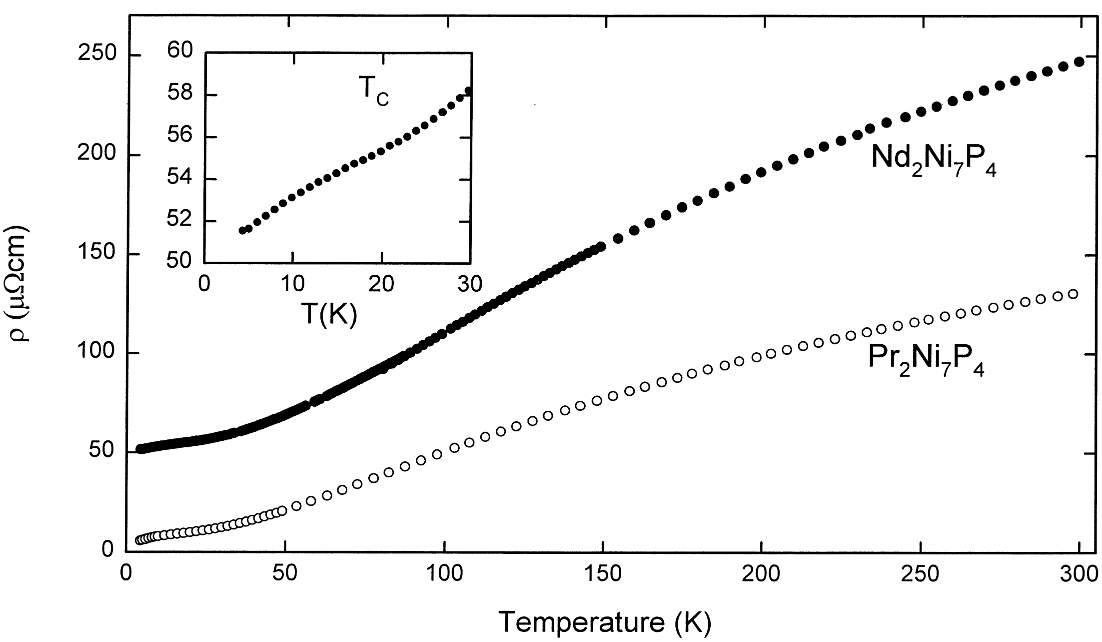

Fig. 7. Electrical resistivity versus temperature for $Pr_2Ni_7P_4$ and $Nd_2Ni_7P_4$. Inset: low temperature part of $\rho(T)$ for $Nd_2Ni_7P_4$, enlarged scale.

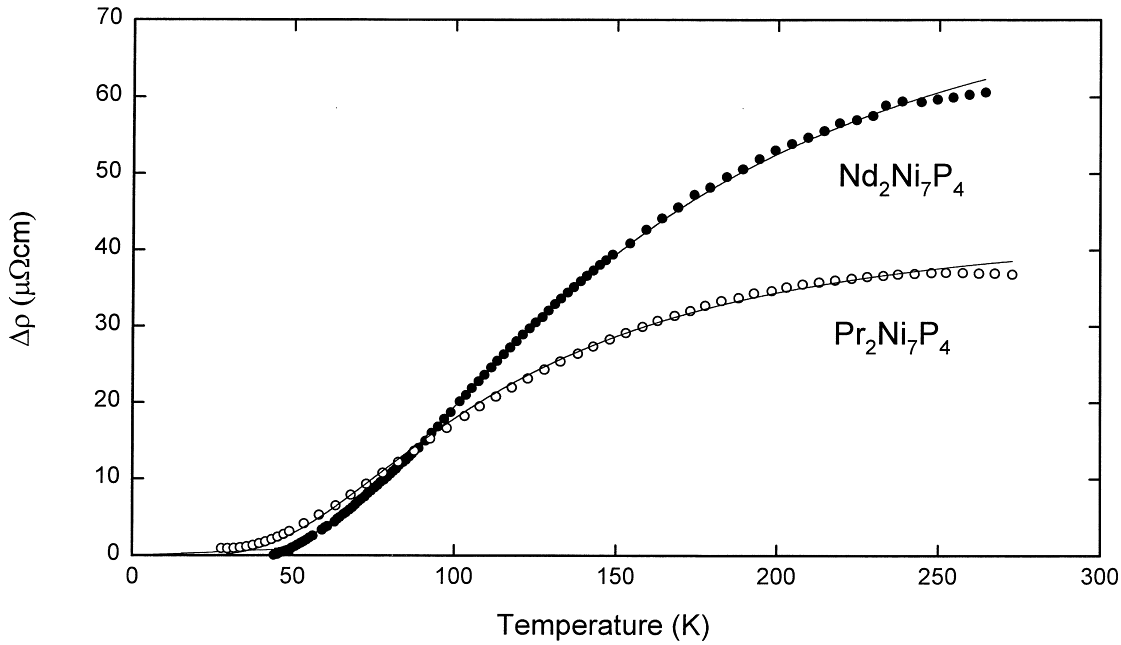

Fig. 8. Temperature dependence of the crystalline field split contribution $\Delta\rho$ of the resistivity after subtracting the residual and the phonon term from the total resistivity (Eq. (3)) for $Pr_2Ni_7P_4$ and $Nd_2Ni_7P_4$. Solid line: calculation according Eq. (4).

get a rough estimate of $\rho_{SPD}(T)$ by graphical extrapolation [7]

$$\Delta\rho = \rho_{SPD}(T) = \rho(T) - \rho_o - \rho_{ph}(T) \qquad (3)$$

and the obtained graphs are shown in Fig. 8. We associate these extra contributions with the interactions of the conduction electrons and the crystalline field split levels of the $^3H_4$ 9-fold degenerate Pr^{3+} and the $^4I_{9/2}$ 10-fold degenerate Nd^{3+}ground state in $Pr_2Ni_7P_4$ and $Nd_2Ni_7P_4$, respectively. Not knowing the exact level scheme, we use a single spacing, δ, crystal field model [8] for an order of magnitude estimate. A least-squares fit according to the equation

$$\Delta\rho = \rho_{CF}(T) = \Delta\rho_{CF}(\infty)\frac{1}{\cosh^2(\delta/2kT)} \qquad (4)$$

provides a good description of the experimental data up to 300 K, as shown by the solid lines in Fig. 8 and leads to a crystal-field splitting of the first excited ‘multiplet’ of 205 K ($\Delta\rho_{CF}(\infty) = 44$ $\mu\Omega$ cm) and 265 K ($\Delta\rho_{CF}(\infty) = 79$ $\mu\Omega$ cm), respectively.

Acknowledgements

This research has been sponsored in part by the Austrian Science Foundation (FWF) under grant P 12843-CHE. V. B. is grateful to the FWF providing a Lise Meitner fellowship M546-CHE.

References

[1] Y. Kuz’ma, S. Chykhrij, in: K.A. Gschneidner Jr., L. Eyring (Eds.), Handbook on the Physics and Chemistry of Rare Earths, Vol. 23(6), Elsevier, Amsterdam, 1996, p. 285.
[2] S. Chykhrij, Y. Kuz’ma, S. Oryshchyn, B.V. Chabursky, V.S. Fundamentskyy, Dopov. Akad. Nauk Ukr. RSR Ser. B 9 (1990) 49.
[3] V. Babizhetskyy, Y. Kuz’ma, Zh. Neorgan. Khim. 39 (1994) 322.
[4] L.G. Akselrud, Yu.N. Grin, V.K. Pecharsky, P.Yu. Zavalij, CSD-universal program package for single crystal and powder data treatment, in: XIIth Eur. Crystallogr. Meeting, Moscow 3, 1989, p. 155.
[5] N.F. Mott, H. Jones, in: The Theory of the Properties of Metals and Alloys, Oxford University Press, London, 1958.
[6] G. Grimvall, in: The Electron-Phonon Interaction in Metals, North-Holland, Amsterdam, 1981.
[7] E. Gratz, M.J. Zuckermann, in: K.A. Gschneidner Jr., L. Eyring (Eds.), Handbook on the Physics and Chemistry of Rare Earths, Vol. 5, Elsevier, Amsterdam, 1982, p. 137.
[8] T. van Peski-Tinbergen, A.S. Dekker, Physica 29 (1963) 917.